Structure, thermodynamics, and dynamics of the liquid/vapor interface of water/dimethylsulfoxide mixtures

Ilan Benjamin[a)]
Department of Chemistry, University of California, Santa Cruz, California 95064

(Received 12 November 1998; accepted 25 January 1999)

Molecular dynamics computer simulations are used to study the structure, thermodynamics and dynamics of the liquid/vapor interface of water/DMSO (dimethylsulfoxide) mixtures. Both the infinite dilution limit (single DMSO molecule) and four different finite concentration mixtures are investigated. Considered are the potential of mean force for the adsorption of DMSO and the dependence of several surface structural properties (orientation, hydrogen bonding) and surface potential on the bulk concentration of DMSO. The adsorption dynamics are also investigated and compared with a diffusion model. In general, the results are in good agreement with recent experimental measurements. © *1999 American Institute of Physics.* [S0021-9606(99)50116-5]

I. INTRODUCTION

The liquid/vapor interface of water-dimethylsulfoxide [$(CH_3)_2SO$, DMSO] mixtures is a system of much current interest at both the practical and fundamental levels. DMSO is an intermediate in the process which leads to the formation of sulfuric acid in atmospheric aerosols.[1] Understanding the structure and thermodynamics of the water/DMSO liquid/vapor interface as a function of bulk composition is prerequisite for understanding the reactivity of DMSO.

DMSO is also one of the most widely used aprotic polar solvents in electrochemistry,[2] and its adsorption on metal surfaces has been extensively studied.[3] These studies underscore the importance of understanding the structure of interfacial DMSO for understanding double layer phenomena at both the metal/DMSO interface and the free surface of water/DMSO.

The surface of water/DMSO mixtures is also interesting at the fundamental level because the unusual properties of the bulk mixtures are expected to show up in their unique surface behavior. One end of the DMSO molecule is a strong proton acceptor and can hydrogen-bond with water. The other end experiences a weak hydrophobic hydration. The water/DMSO mixtures exhibit extreme deviations from ideal behavior, and this has been attributed to the hydrophobic association of the DMSO molecules.[4] However, recent molecular dynamics simulations of bulk aqueous solutions of DMSO and neutron scattering experiments do not show any evidence for association, but do demonstrate the enhancement of water–water hydrogen bonding.[5–7] It would be very interesting to examine how this behavior may be modified at the interface.

Despite the importance of DMSO in atmospheric and electrochemical processes, the adsorption of this molecule at water surfaces has only recently been investigated experimentally. Trasatti and coworkers have studied the adsorption of DMSO at the free surface of aqueous solutions by a combination of surface tension and surface potential measurements.[8] From these measurements, a model for the structure of this interface has been proposed. Nonlinear spectroscopic techniques that have been extensively used in recent years to study the structure of aqueous interfaces[9,10] have very recently been applied to the study of the free surface of mixtures,[11,12] and in particular to the water/DMSO surface. Resonance-enhanced surface second harmonic generation (SHG) has been used by Karpovich and Ray to measure the adsorption of DMSO at the water liquid/vapor interface and to suggest a potential energy profile for the uptake of this molecule by water surfaces.[13] Allen, Gragson, and Richmond have used surface sum frequency generation (SFG) to measure, in addition to the adsorption isotherm, several structural properties of the surface of water/DMSO mixtures.[14] All of the above studies indicate that the surface region is rich in DMSO relative to the bulk. Such surface partitioning effects have been found in other fully miscible water/polar liquid mixtures.[11,15]

There is only one theoretical treatment of the interface of water/DMSO mixtures—a mean-field model by Luzar,[16] and no molecular dynamics calculations, although several molecular dynamics simulations of the liquid/vapor interface of other aqueous solutions have been reported.[17–19] Luzar focused on the contribution of hydrogen bonds to the bulk and surface properties of water/DMSO mixtures.[16] The model gave information about the density profiles and hydrogen bonding as a function of the distance from the interface and was in reasonable agreement with experimental data on surface excess properties over the entire concentration range.[16] Tarek, Tobias, and Klein[18] have examined using molecular dynamics simulations for the structure and dynamics of the liquid/vapor interface of a 0.1 M ethanol–water solution and observed the segregation of ethanol at the surface, in agreement with experiments. However, ethanol is quite similar to water in its ability to serve as both proton donor and acceptor. In addition, no attempt has been made to study the interface structure as a function of bulk concentration, and the length of the simulations was too short to observe certain dynamical properties, as will be demonstrated in the system

a)Electronic mail: ilan@scib.ucsc.edu

discussed in this paper. Pohorille and Wilson computed the potential of mean force for the transfer of a single ethanol molecule across the water liquid/vapor interface and showed that there is no barrier to desorption into the bulk.[19]

In this work, we provide a comprehensive treatment of the structure and dynamics of the surface of water/DMSO mixtures. We examine both the single molecule properties, such as the potential of mean force, and the finite concentration equilibrium properties. Special attention is given to the problem of the rate at which surface properties attain their equilibrium values. We believe that a discussion of nonequilibrium steady state processes, such as the uptake of species by water surfaces (under certain experimental conditions), phase separation, and electrode processes, requires an understanding of these time-scales.

This paper is organized as follows: In Sec. II, we briefly describe the molecular systems and discuss the potential energy functions used in the simulations. In Sec. III, we discuss the results, with special attention to the time-development of the interface structure. In Sec. IV, we present our summary and conclusions.

II. SYSTEMS AND METHODS

A. Potential energy functions

The DMSO molecule is represented by four atomic sites (each methyl group is approximated by a united atom of mass 14). Our model for the intermolecular interactions between DMSO molecules is the P2 model developed by Luzar and Chandler.[6] This model is in good agreement with neutron diffraction experiments on bulk water/DMSO mixtures over a wide concentration range.[7] The potential is represented by a sum of pairwise Coulomb and 6–12 Lennard-Jones interactions

$$u_{ij}(r)=4\epsilon_{ij}[(\sigma_{ij}/r)^{12}-(\sigma_{ij}/r)^{6}]+\frac{q_iq_j}{r}, \tag{1}$$

where r is the distance between sites i and j in different molecules, q_i is the charge assigned to site i, and σ_{ij} and ϵ_{ij} are determined from the Lennard-Jones parameters of the different sites according to the ''mixing'' rule

$$\sigma_{ij}=\tfrac{1}{2}(\sigma_i+\sigma_j), \quad \epsilon_{ij}=\sqrt{\epsilon_i\epsilon_j}. \tag{2}$$

The parameters q_i, σ_i, and ϵ_i for the oxygen, sulfur, and methyl sites in the DMSO molecule are given in Table I.

Unlike most of the existing interaction potential models of DMSO, ours is flexible. The intramolecular vibrational potential is represented by harmonic bond stretching and angle-bending terms. The force constants and the equilibrium bond lengths and bond angles are also given in Table I.

The water model is the flexible SPC (single point charge) model used previously to study the properties of interfacial water. It is also represented by a sum of pairwise Coulomb and 6–12 Lennard-Jones interactions with parameters given in Table I. The water intramolecular potential is a fit to the spectroscopic data of gas phase water.[20] The water-DMSO interactions are also represented by the model given by Eq. (1) and the mixing rule [Eq. (2)].

TABLE I. (a) Lennard-Jones parameters and partial charges for water and DMSO. (b) Intramolecular harmonic force field parameters for DMSO.

Atom	σ (Å)	ϵ (kJ/mol)	Q (a.u.)
	(a)		
S	3.4	1.00	0.139
O(DMSO)	2.8	0.30	−0.459
CH_3	3.8	1.23	0.160
O (water)	3.165	0.65	−0.82
H (water)	0.0	0.00	0.41
	(b)		
k_{S-O}		2510 kJ/mol Å^{-2}	
r_{S-O}		1.53 Å	
k_{S-C}		1670 kJ/mol Å^{-2}	
r_{S-C}		1.80 Å	
k_{C-S-C}		840 kJ/mol rad^{-2}	
q_{C-S-C}		97.4°	
k_{C-S-O}		840 kJ/mol rad^{-2}	
q_{C-S-O}		106.75°	

B. Free energy calculations at infinite dilution

An important thermodynamic characterization of the adsorption of a solute at the interface is the potential of mean force $A(z)$ as a function of the distance z of the solute center of mass along the normal to the interface. Adsorption at the interface corresponds to a minimum in $A(z)$ for z near the interface. The value of $A(z)$ relative to the bulk value gives the adsorption free energy of the solute. The location $z_{\min^-}$ of this minimum gives important insight about the solvation at the interface. For nonspherical solute molecules, the $A(z)$ may be a function of the solute orientation.

$A(z)$ can be evaluated using a variety of techniques.[21] We use here the umbrella sampling procedure.[22] The simulation box is divided into a number of thin slabs parallel to the interface. The position and width of each slab is selected so that they overlap in the z direction. In each slab, the solute is allowed to move freely in the x,y directions, but it is restricted in the z direction by a continuous potential of the form

$$U_{\text{slab}}(z)=\begin{cases} k(z-z_+)^3, & z\geqslant z_+ \\ 0, & z_-<z<z_+ \\ k(z-z_-)^3, & z\leqslant z_-, \end{cases} \tag{3}$$

where k determines the steepness of the ''soft'' walls restricting the solute to the region $[z_-,z_+]$. A simulation run that is long enough for the solute to significantly sample the whole $[z_-,z_+]$ interval of each slab allows one to obtain an accurate probability distribution $P_n(z)$ for the solute in the n'th slab, from which the potential of mean force can be calculated using

$$A_n(z)=-kT\ln P_n(z)+C_n. \tag{4}$$

The constant C_n can be determined from the condition that $A(z)$ is continuous over the whole region of z values. This is done by a least-square fit of the functions $A_n(z)$ and $A_{n+1}(z)$ for the values of z corresponding to the region where slabs n and $n+1$ overlap. The simulation run in each slab gives additional structural information, such as solute orientation,

TABLE II. Summary of system sizes and other properties.

System	Number of water molecules (N_{Water})	Number of DMSO molecules (N_{DMSO})	DMSO mol fraction (x_{DMSO})	Location of Gibbs surface (z_G) (Å)
A	972	51	0.05	16.5
B	920	103	0.10	18.9
C	870	153	0.15	20.8
D	818	205	0.20	23.1

which enables the study of the variation of such properties as a function of the DMSO position along the interface normal.

C. Mixture simulations

We consider four water/DMSO mixtures A, B, C, D corresponding to the mol fractions of DMSO 0.05, 0.1, 0.15, and 0.20, respectively. The mixtures are prepared by starting with a slab of bulk water in equilibrium with its own vapor, containing a total of 1023 water molecules in a box of dimensions $3.128\times3.128\times10$ nm (the interface is perpendicular to the long axis). Each one of the mixtures is prepared by replacing the proper number of randomly selected water molecules by DMSO molecules as listed in Table II. The water molecules are selected from the bulk region only. Thus, each system initially contains zero DMSO molecules at the interface. After a relatively short equilibration period of 200 ps, each system is simulated using a constant temperature run for 3 ns. A number of structural properties are followed as a function of time by performing averages over 0.25 ns intervals. Equilibrium averages are computed over the last time interval in which no further change is observed as a function of time. This gives information about the time evolution of any property and its final equilibrium value.

D. Other simulation details

In all cases, the integration time step is 1 fs and the temperature 300 K. The total of 26 ns trajectories took 2 months of cpu time on a 6-processor SGI ORIGIN 2000 workstation.

III. RESULTS AND DISCUSSION

A. Potential of mean force

The potential of mean force for the transfer of a single DMSO molecule from bulk water to the water liquid/vapor interface (the system includes 1023 water molecules) is calculated using 7 overlapping slabs of a width of 3 Å each, spanning a distance of 15 Å (so that each slab has a 1 Å overlap with each of its neighboring slabs). In each slab, a constant temperature trajectory of length 2 ns is performed. This provides enough statistical sampling to give an accurate result.

The results of these calculations are summarized in Fig. 1. The top panel (A) shows the density profile of the water slab. Indicated is the interval [2–17 Å] along the normal to the interface (the Z direction) in which the umbrella sampling calculations are done. The Gibbs dividing surface which is used as one measure of the surface ''location'' is

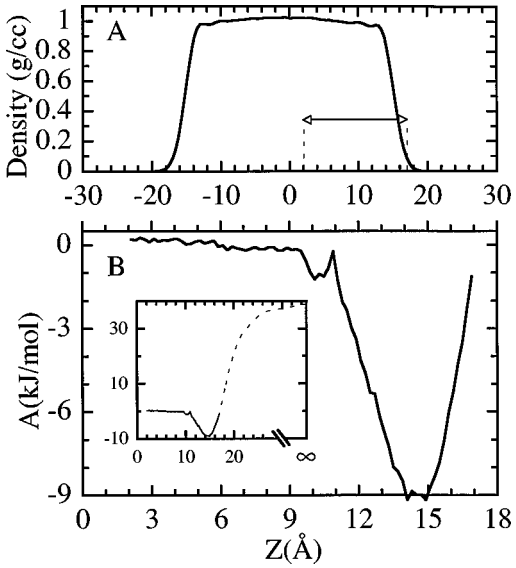

FIG. 1. (A): Density profile of water in the system used to compute the DMSO potential of mean force ($T=300$ K here and in all of the figures below). Indicated is the region where the umbrella sampling is performed. (B): The potential of mean force for DMSO adsorption at the water liquid/vapor interface. The inset shows the schematic continuation of the potential of mean force to the gas phase based on the computed value of the solvation free energy of DMSO.

defined as the plane where the excess molecules on the vapor side balance the reduction on the bulk side. It is around 15 Å, where the water density is approximately 50% of its bulk value.

Panel B shows the potential of mean force obtained by merging the data from the 7 windows. Despite the considerable length of the trajectories, the sampling of every section of each window is quite slow. Thus, the uncertainty in the free energy profile (calculated by dividing the data from each window into 10 groups) is quite large—2 kJ/mol. The data suggest that DMSO is surface-active—the adsorption free energy is -9 kJ/mol, which is in reasonable agreement with the experimental data of Dabkowski *et al.*[8] (-9.8 kJ/mol) and of Karpovich and Ray[13] (-11.8 ± 1.2 kJ/mol), but smaller than that reported by Allen, Grayson, and Richmond[14] using SFG measurements (-15 kJ/mol) or surface tension measurements (-19.8 kJ/mol). One reason for these discrepancies between the simulations and the various experiments is the fact that the experimental data are derived from finite concentration measurements and are based on a fit to the adsorption isotherm. Of course, there is always the possibility that the DMSO/water potentials which were optimized to bulk structural data are not accurate for interfacial simulations. However, the water/DMSO potential seems adequate, as the solvation free energy of DMSO in bulk water calculated from a separate bulk thermodynamic integration calculation yields a value of -39 kJ/mol, which is in good agreement with the experimental value of -36 kJ/mol.[13]

The potential of mean force remains flat up to a distance of about 5 Å from the Gibbs surface. At this point, it begins to decrease monotonically (the small barrier near $z=11$ Å is within the statistical error) towards the minimum, which is located very close to the location of the Gibbs surface. Com-

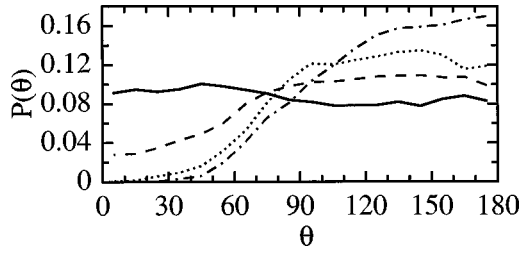

FIG. 2. The probability distribution for the angle θ between the normal to the water liquid/vapor interface and the SO vector of DMSO. $\theta=0°$ correspond to the oxygen pointing away from the bulk. The different curves correspond to calculations performed in slabs of width 3 Å that are centered at different locations along the interface normal. Solid line: bulk calculations; Dashed line: 4 Å below (into the bulk) the Gibbs surface; Dotted line: 2 Å below the Gibbs surface; Dashed–dotted line: at the Gibbs surface.

bining this data with the previously mentioned solvation free energy of -39 kJ/mol allows one to draw schematically the complete free energy surface for the uptake of DMSO by water. This is shown in the inset of panel B. It suggests that a DMSO molecule does not experience an overall barrier on its way to the bulk. However, the calculations indicate that solvated DMSO at the interface is a global free energy minimum state and the molecule must be supplied with 9 kJ/mol of free energy if it is to be transferred to the bulk. Thus, the observed rate for the process DMSO(surface)→DMSO(bulk) must be much slower than the rate predicted from the diffusion rate of DMSO.

Finally, the simulations in each window allow one to obtain several structural properties, and Fig. 2 shows one property which has been the subject of recent experimental interest. This figure shows the probability distribution for the angle between the S–O vector (bisector of the CSC angle) of DMSO and the normal to the interface for several distances from the interface. It is clear that there is a significant tendency for the DMSO molecule to point its CH_3 groups away from bulk water. Near the Gibbs surface there is almost zero population of inverted orientations (i.e., CH_3 pointing towards bulk water). As one gets closer to the bulk (but still in the region where the local free energy of adsorption is negative), there is a small but statistically meaningful population of inverted orientations that allows one to calculate the free energy difference for a 180° rotation of the DMSO molecule. It is found to be about 3 kJ/mol. This number will be significantly larger if the molecule is rotated closer to the surface, and it should therefore be regarded as a lower limit to the true cost of rotating the molecule at the interface. The result of this is a relatively stable hydrophobic ''coating'' of the water surface, which may have important atmospheric implications.[14] We will return to this issue when we examine below the orientations at the surface of water/DMSO mixtures.

An interesting issue to consider is the factors that determine the orientational preference for the DMSO molecules at the interface. A simple argument used in the literature in this and other cases is that the orientational preference reflects the hydrophobic nature of the CH_3 group. However, it is likely that the strong directional character of the water-DMSO hydrogen bonding, together with the water orientational preference, will also contribute to the specific DMSO orientation. Unfortunately, there is no way of separating these two factors, especially when one considers that the hydrophobic effect is largely a reflection of the tendency of the system to minimize the disruption of water–hydrogen bondings, which in this system may well be accomplished by enhanced water-DMSO hydrogen bonding at the interface.[16] We discuss hydrogen bondings in more detail later.

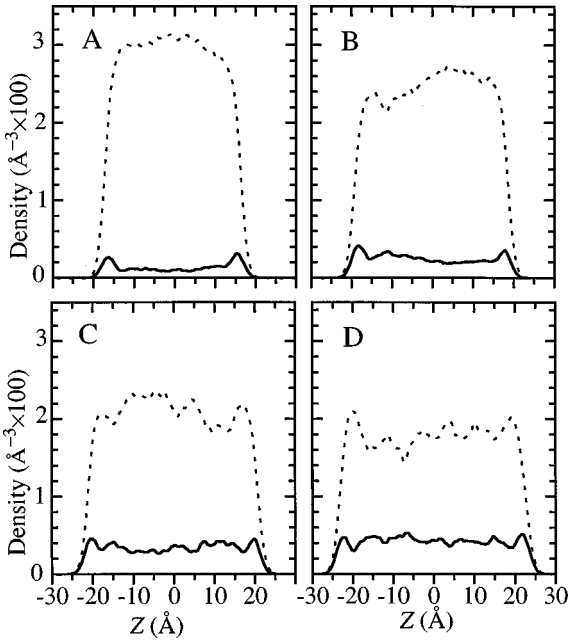

FIG. 3. Density profiles of water (dashed lines) and of DMSO (solid lines) in the four mixtures. The DMSO overall mol fractions are 0.05 (A), 0.1 (B), 0.15 (C), and 0.2 (D).

B. Water/DMSO mixtures: equilibrium surface structure

Experimental studies of the surface properties of water/DMSO solutions are done with finite (and sometimes quite large) bulk DMSO concentrations. In this section, we discuss the equilibrium surface properties of four different water/DMSO mixtures with DMSO mol fractions of 0.05, 0.1, 0.15, and 0.2 (systems A–D, respectively). We focus on data that is directly or indirectly accessible to experimental determination and compare the results, when appropriate, to the results of the single DMSO molecule discussed in the preceding section.

1. Density profiles

Figure 3 shows the density of water and of DMSO as a function of the distance normal to the interface for the four different systems. For each system, the density is calculated from the configurations obtained during the last 1 ns of the 3 ns trajectory. In all systems, one clearly observes an excess density of DMSO near the water Gibbs surface, and some depletion when one moves towards the bulk. The locations of the Gibbs surfaces are given in Table II. Note that the Gibbs surface calculated with respect to the water density is in different z values, because the total volume of the system changes as we increase the DMSO concentration with a fixed

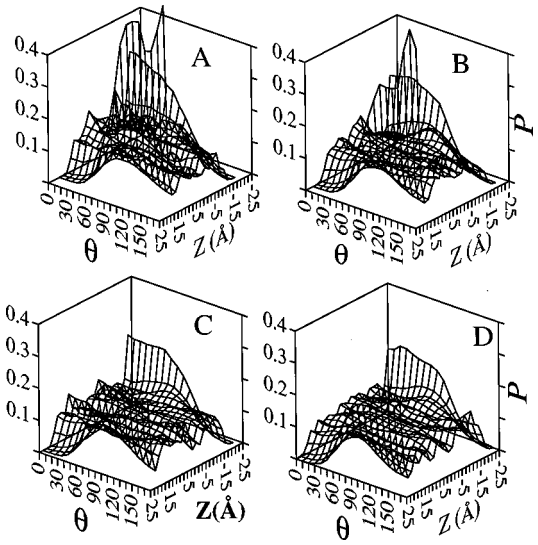

FIG. 4. The probability distributions for the angle θ between the vector pointing from the sulfur to the oxygen atom of DMSO and the interface normal as a function of the distance Z along the interface normal for the four water/DMSO mixtures, as listed in Fig. 3.

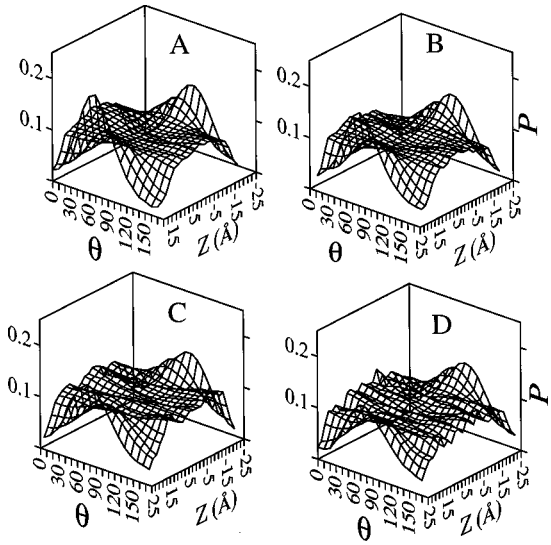

FIG. 5. The probability distributions for the angle θ between the water dipole and the interface normal as a function of the distance z along the interface normal for the four water/DMSO mixtures A–D.

total number of molecules. This DMSO surface excess is consistent with the fact that the DMSO potential of mean force has a global minimum at the water Gibbs surface, and it is in agreement with a variety of different experiments cited in the introduction. Similar results have been observed in simulations of water/ethanol mixtures.

The density profile of DMSO in systems A and B (low concentrations) is quite smooth, whereas in systems C and D (larger concentrations of DMSO) one observes a noisier profile despite the fact that there are more DMSO molecules. The water density is also less smooth, and it is approximately locally larger when the corresponding DMSO density is locally lower, and vice versa. This suggests that there is local clustering of DMSO molecules and water molecules in the higher concentration systems. These clusters drift around so that when the number of configurations included in the average is increased, a less noisy profile is obtained. This was confirmed by computing the average densities over a period of 2 ns. The observed local clustering seems to contradict the results of the neutron scattering data mentioned earlier.[7] However, this reference also suggests that some clustering of DMSO molecules is possible via their oxygen atoms. A recent simulation by Borin and Skaf[23] suggests that this association could be the result of water-DMSO hydrogen bonding where a water molecule acts as a bridge between two DMSO molecules.

2. DMSO orientations

The probability distributions for the angle θ between the vector pointing from the sulfur to the oxygen atom of DMSO as a function of the distance z along the interface normal are shown in Fig. 4. The four panels correspond to the systems A–D. The distributions are calculated from the last 1 ns time interval of the 3 ns trajectory for each system. Note that $z=0$ Å is the middle of the bulk region, and $z=\pm S_G$ are the two Gibbs surfaces (defined with respect to water, and given in Table II). It is clear that as in the case of a single DMSO molecule, there is a tendency for the DMSO to point its CH_3 groups away from the bulk, in agreement with recent SFG experiments.[14] The shape of the distribution near the interface is interesting: There is a broad peak near 90° with a slow drop for angles above 90° and a sharp drop for angles below 90° such that the average orientation is around 120°. This corresponds to the transition dipole being near 60° from the normal, in good agreement with experiment. It is also evident that this orientational preference is independent of bulk concentration—the graphs for the different systems are almost identical given the statistical error (which is larger in the system with fewer DMSO molecules).

3. Water orientations

We next consider the orientation of the water molecules at the interface. Figure 5 gives the probability distribution for the angle θ between the water dipole (the vector pointing from the oxygen to the bisector of the HOH angle) and the normal to the interface. We observe that the water molecules on the bulk side of the Gibbs surface have their dipoles parallel to the surface, whereas the molecules on the vapor phase of the Gibbs surface have their dipoles pointing slightly toward the vapor side. We also note that the distributions are slightly concentration-dependent, with the peaks being more pronounced when the DMSO concentration is lower.

Additional orientational information is presented in Fig. 6, where the probability distribution for the orientation of the OH bonds is shown. For water molecules on the bulk side of the Gibbs surface, the distribution exhibits a single broad peak at 90°. Taken together with the information on the dipole orientations given in Fig. 5, this suggests that the HOH plane is parallel to the interface. For water molecules on the vapor side of the Gibbs surface, the distribution exhibits two peaks, one near the interface normal and one near the 90° angle to the interface normal. Taken together with the infor-

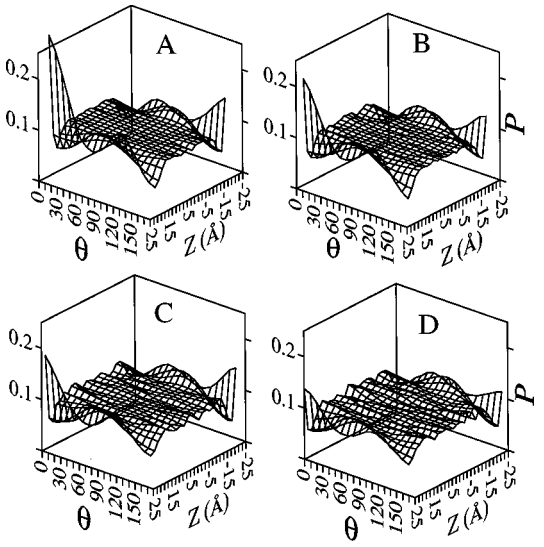

FIG. 6. The probability distributions for the angle θ between the water OH bond and the interface normal as a function of the distance z along the interface normal for the four water/DMSO mixtures A–D.

mation on the dipole orientations given in Fig. 5, this suggests that one of the OH bonds is perpendicular to the interface, and one points slightly toward the bulk. The dependence of water's OH orientation on the concentration is even more pronounced: The peak representing the free OH bond increases as the DMSO concentration decreases.

4. Surface potential

One of the relatively well investigated properties of the water/DMSO liquid/vapor interface is the surface potential. The shift in the surface potential to more negative values upon increase in the DMSO bulk concentration indicates that the DMSO molecules are adsorbed with their CH_3 groups pointing towards the exterior of the liquid phase,[8] in agreement with the more recent spectroscopic data and the molecular dynamics results presented earlier. Measurement of the surface potential of water DMSO mixtures also indicates that in the low concentration range (0–0.05 mol fraction), the potential drop increases with an increase in the DMSO concentration. However, above this concentration range there is a plateau. Although statistical uncertainties prevent us from examining the very low concentration range, it is nevertheless important to see if the molecular dynamics calculations indeed predict this saturation and provide additional insight.

Calculation of the surface potential in molecular dynamics simulations is straightforward.[21] The electric potential difference $\Delta\chi$ across the interface is determined by a numerical integration of the one-dimensional Poisson equation:[24]

$$\Delta\chi = -\frac{1}{\epsilon_0}\int q(z')(z-z')dz', \tag{5}$$

where $\epsilon_0 = 8.854\times10^{-12}\,\text{coulomb}\,\text{V}^{-1}\,\text{m}^{-1}$ is the vacuum permitivity. The charge density profile is defined by $q(z) = \Sigma_i \rho_i(z) Q_i$ and is calculated from the atomic densities $\rho_i(z)$ and the partial charges on the atoms Q_i. From Eq. (5), it is clear that the total potential drop can be partitioned into contributions from the two different liquids. The results for the four water/DMSO mixtures are shown in Fig. 7.

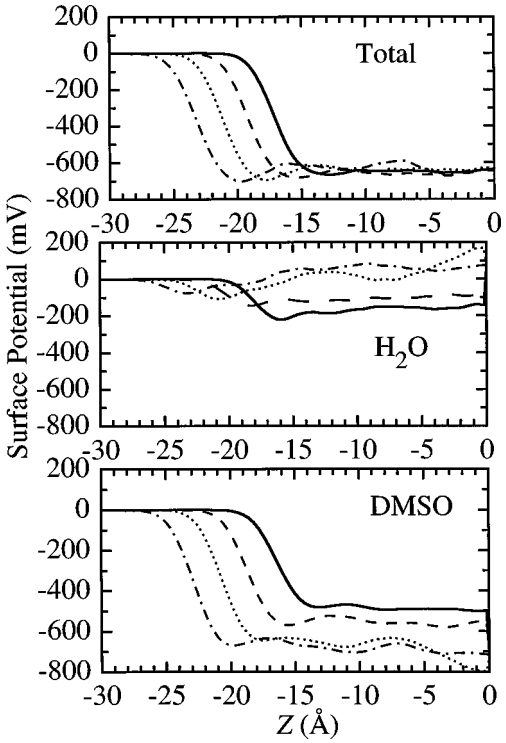

FIG. 7. The surface potential drop as a function of the distance along the interface normal for the water/DMSO mixtures. Top panel: the total potential drop; Center panel: the contribution of water molecules to the total drop; Bottom panel: the contribution of DMSO. In each panel, the solid, dashed, dotted, and dashed–dotted lines correspond to systems A, B, C, D, respectively.

The top panel shows the total surface potential relative to the gas phase (0 Å corresponds to the middle of the slab, i.e., the bulk region), and the middle and bottom panels show the individual contributions of the water and the DMSO, respectively, for each of the four systems. Note that because of the different locations of the surface in the four systems (due to the different volume), the initial drop occurs at different z values, but otherwise the shape and the total potential drop is very similar. The individual contributions of the two liquids show that most of the potential drop is due to the DMSO molecules. It increases from 500 to 700 mV as the concentration of the DMSO increases from 0.05 to 0.2 mol fraction. The water contribution is in the region of ±150 mV. The fact that the water contribution is larger as the DMSO concentration is lower explains the weak dependence of the total potential drop on the composition in this concentration range, which is in qualitative agreement with experiments. However, the major conclusion here is that the potential drop reflects the saturation of the surface region by DMSO molecules, a point that will be further discussed below.

5. Hydrogen bonding

Finally, we consider water–water hydrogen bonding, which although not amenable to direct experimental measurement is nevertheless an interesting indicator of the inter-

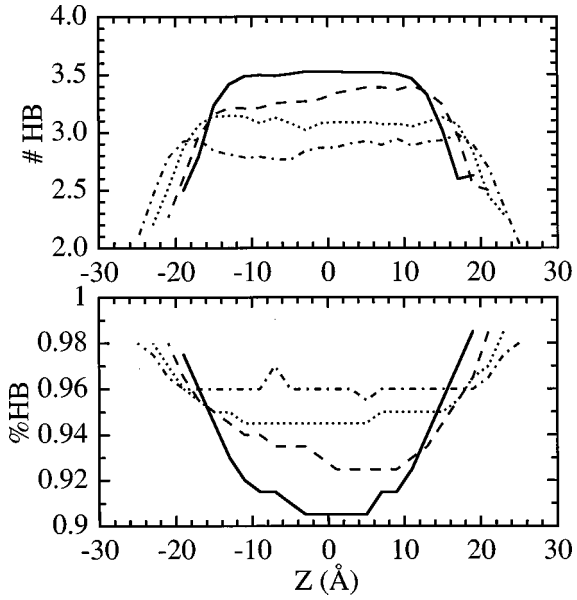

FIG. 8. Top panel: number of hydrogen bonds per water molecule (as defined in the text) as a function of the location along the interface normal for the four water/DMSO mixtures. Bottom panel: the number of hydrogen bonds per water molecule divided by the coordination number of water. In each panel, the solid, dashed, dotted and dashed–dotted lines correspond to systems A, B, C, D, respectively.

face structure. We consider two water molecules to be hydrogen-bonded if their pair interaction energy is more negative than -10 kJ/mol. It is also possible to have a structural definition where the distance between two oxygen atoms and the OHO angle are used, but the results are very similar to what is discussed later. The top panel of Fig. 8 shows the total number of hydrogen bonds per water molecule as a function of the position along the interface normal for the four different systems. In the bulk region, this number is independent of location and decreases as the DMSO concentration increases as expected. In addition, for each system, this number monotonically decreases as the Gibbs surface is crossed. This effect is clearly explained by the fact that the number density of water is reduced near the interface.

A more interesting quantity is obtained when the number of hydrogen bonds per water molecule is divided by the water–water coordination number. This gives information about the probability of any hydrogen bond existing. The bottom panel of Fig. 8 shows that in the bulk region this probability increases as the DMSO concentration increases: The water–water hydrogen bonding is enhanced by the presence of the DMSO molecules. This is similar to results obtained by molecular dynamics simulations of bulk water/DMSO mixtures.[5] The new feature here is that the effect introduced by the interface becomes more pronounced as the DMSO concentration is reduced. For example, at the highest DMSO concentration, the water–water hydrogen bonding is almost unaffected as the interface is approached. This behavior makes sense when taken together with results from several molecular dynamics studies of water/organic liquid interfaces and water liquid/vapor interfaces.[25] It has been found that the probability that any hydrogen bond exists *goes up* from about 0.8 in bulk water to 0.9 at the interface. Thus, at high DMSO concentrations, the water–water hydrogen bonding is already quite strong in the bulk, and as the interface is approached, not much more enhancement is possible.

The results presented here support the basic assumptions of the mean field model for water/DMSO mixtures developed by Luzar.[16] In this model, water-DMSO hydrogen bonding leads to a decrease in the number of water/water hydrogen bonding as the concentration of DMSO is increased. The surface is described as a region of one molecular layer in which the number of water–water hydrogen bonds is smaller than in the bulk. Although the molecular dynamics suggest that the interface region is wider, the molecular model, unlike the mean field model, includes the contribution of capillary waves which broaden the interface. Luzar found the density profile by minimizing the free energy of the systems given the above assumptions. Direct quantitative comparison with the density profiles of Fig. 3 is not possible because the mean field model imposes a sharp cut-off on the number density at the interface.

C. Nonequilibrium dynamics

One of the issues that has received very little attention in molecular modeling of liquid interfaces is the rate at which equilibrium properties are established. Besides the fundamental interest in this dynamic property, a knowledge of this rate is useful for two main reasons. First, the calculation of many surface properties in molecular dynamics simulations follows an equilibration period starting from a nonequilibrium density distribution. It is important to establish the minimum length of such an equilibrium run. Second, and more importantly, several processes of electrochemical and atmospheric interest involve the diffusive transport of solute molecules across the interface under conditions of nonequilibrium initial density distribution. The systems considered in this work allow us to examine the rate of this transport process as a function of (the average) bulk concentration. In this section, we consider the rate of establishment of the equilibrium value for several structural properties discussed in the previous section.

1. Surface excess

We first consider the actual mass transport of DMSO. The system starts with no DMSO molecules at the interface, and in order to establish equilibrium, these molecules must diffuse to the interface. Rather than follow the number density at the interface, we follow the standard thermodynamic property of surface excess. It is defined as follows:[26]

$$\Gamma = \frac{N_{\mathrm{DMSO}} - \rho_{\mathrm{bulk}} V}{S}, \tag{6}$$

where N_{DMSO} is the total number of DMSO molecules, ρ_{bulk} is the bulk number density of DMSO (calculated from the number of DMSO molecules in the region between -10 and 10 Å), V is the volume enclosed by the two Gibbs dividing surfaces at $\pm S_G$, and S is the surface area. Thus, Γ gives the surface density in excess of what is expected if the bulk density is uniform up to the Gibbs surface. Our initial (nonequilibrium) density profile corresponds to a large negative

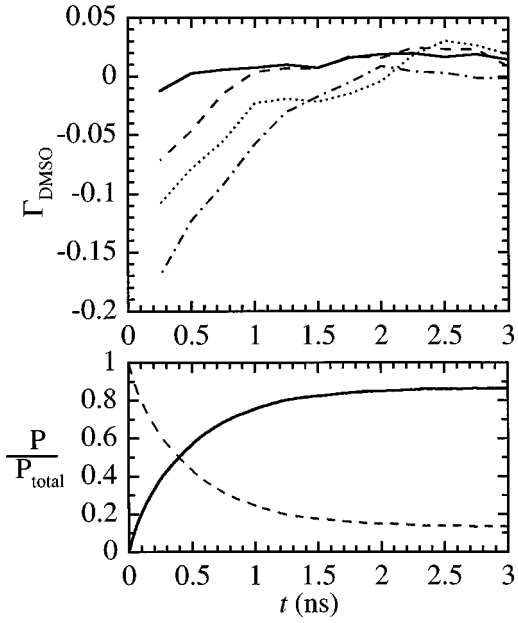

FIG. 9. Top panel: The surface excess of DMSO (defined in the text) as a function of time for the four water/DMSO mixtures starting from an initial distribution where all the DMSO molecules are in the bulk region (between −10 and 10 Å). The solid, dashed, dotted, and dashed–dotted lines correspond to systems A, B, C, D, respectively. Bottom panel: The numerical solution of the diffusion equation for a particle diffusing on the potential of mean force of Fig. 1(B). Solid line: the integrated probability distribution in the surface region (defined in the text); Dashed line: the same for the bulk region.

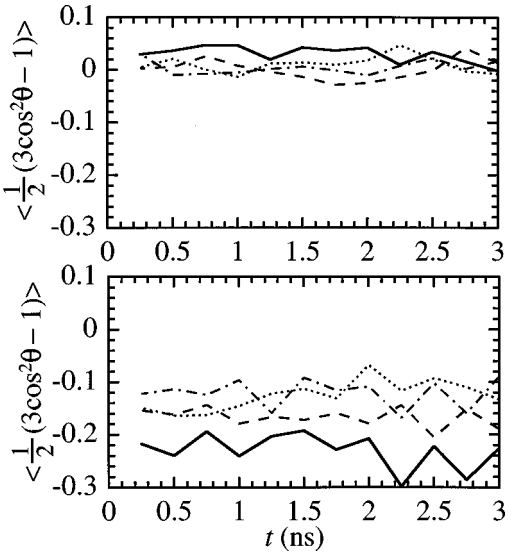

FIG. 10. Water dipole orientation order parameter as a function of time following the evolution towards equilibrium in the four water/DMSO mixtures. The solid, dashed, dotted, and dashed–dotted lines correspond to systems A, B, C, D, respectively. Top panel: bulk region; Bottom panel: interface region.

value of Γ. As time progresses, Γ increases as DMSO molecules transfer to the interface. We expect Γ to be slightly positive at equilibrium, which is consistent with the positive adsorption of DMSO. This is indeed the case, as shown in Fig. 9, where $\Gamma(t)$ is plotted for the four systems. Note that the final values are quite similar to each other and in agreement with the experimental information available at the 0.05–0.2 mol fraction concentration range. Because the actual number of molecules is quite small, it is not possible to quantitatively relate these values of Γ to the adsorption free energy (in order to compare them with the potential of mean force which corresponds to infinite dilution), but the saturation suggests significant interactions between interfacial molecules.

Next we consider the time dependence of Γ. The main theoretical question we wish to address here is whether the approach to equilibrium can be modeled by a one-dimensional diffusion in an external field, with the field being the potential of mean force calculated earlier. To examine this issue we solve (for technical details see Ref. 27) the following equation numerically:

$$\frac{\partial p(z,t)}{\partial t}=D\frac{\partial^2 p(z,t)}{\partial z^2}+\frac{D}{kT}\frac{\partial}{\partial z}\left[p(z,t)\frac{\partial A(z)}{\partial z}\right], \tag{7}$$

where $D=10^{-5}\,\mathrm{cm}^2/\mathrm{s}$ is the DMSO diffusion constant in water (assuming it to be independent of z), and $A(z)$ is the potential of mean force given in Fig. 1(B). $p(z,t)$ is the probability of finding a DMSO molecule in the region $[z,z+dz]$ at time t. The boundary conditions that most closely correspond to the simulation runs are given by

$$\begin{aligned} &p(|z|<z_B,t=0)=1,\\ &p(|z|>z_S,t=0)=0, \end{aligned} \tag{8}$$

where $|z|<z_B$ is the bulk region ($z_B=10\,\text{Å}$), and z_S is the location where the $A(z)$ just begins to change ($z_S=11\,\text{Å}$). The total surface population is defined by

$$p_s(t)=\int_{|z|>z_S}p(z,t)dz. \tag{9}$$

Given a model for the surface area per molecule, $p_s(t)$ can be directly related to the surface excess. Here we are only interested in an approximate time scale, and a direct examination of $p_s(t)$ will suffice. This quantity is shown in the bottom panel of Fig. 9 (solid line), together with the total bulk concentration $(1-p_s(t))$. Note that the final value is exactly what one expects from the Boltzmann distribution

$$p_s^{\mathrm{eq}}=p_s(t\to\infty)=\frac{\int_{|z|>z_S}\exp[-A(z)/kT]dz}{\int_{-\infty}^{\infty}\exp[-A(z)/kT]dz}, \tag{10}$$

which, given the data in Fig. 1, is equal to 0.865. Clearly, the one-dimensional diffusion model is able to give the correct time scale for the process.

2. Molecular orientation

We next examine the time evolution of the water dipole orientation. For simplicity, we consider the order parameter $\langle\frac{1}{2}(3\cos^2\theta-1)\rangle$ rather than the complete distribution. The top panel shows the bulk and the bottom panel the interface. A value of −1/2 corresponds to a perfect parallel orientation, so the data in the bottom panel, despite the noise, is consistent with the equilibrium distribution shown earlier. The main finding depicted in Fig. 10 is that the water orientation is established very rapidly—there is very little change as a

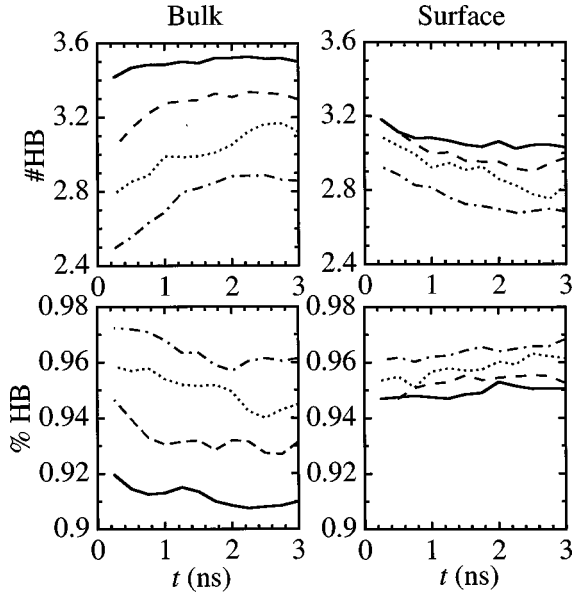

FIG. 11. Water hydrogen-bonding statistics as a function of time following the evolution towards equilibrium in the four water/DMSO mixtures. In each panel, the solid, dashed, dotted, and dashed–dotted lines correspond to systems A, B, C, D, respectively.

function of time in the value of the order parameter. Similar results were found for the DMSO orientations.

3. Hydrogen bonding

Finally, we show in Fig. 11 the time development of the water–water hydrogen bonding. As expected, the initial nonequilibrium density of DMSO in bulk water results in the disruption of water hydrogen-bonding, the disruption being the largest for the most concentrated solution. As the density profile approaches equilibrium, the number of hydrogen bonds per water molecule in the bulk increases on the same time scale as the density (top left panel of Fig. 11). Correspondingly, the number of hydrogen bonds per interfacial water molecule decreases towards the equilibrium value (top right panel). Interestingly, the probability that any hydrogen bond is formed (shown in the bottom two panels) is almost time-independent. This is reasonable if the main change in the local environment of each water molecule involves a change in the hydration number as the density approaches the equilibrium value.

IV. SUMMARY AND CONCLUSIONS

We have presented a comprehensive study of the surface of water/DMSO mixtures. This system exhibits a behavior that resembles other water/miscible liquid mixtures but also shows some novel characteristics. The potential of mean force for the adsorption of DMSO at the surface of water shows that there is a global minimum at the interface which is consistent with the surface excess of DMSO observed in experiments.[8,14] It is also consistent with the surface excess observed in the present finite concentration studies. No barrier to transfer of DMSO to the bulk is observed. The DMSO molecules tend to orient their CH_3 groups away from the bulk in both the infinite dilution and finite concentration simulations, in agreement with SHG experiments and surface potential measurements. The calculations of the surface potential show saturation in the 0.05–0.2 mol fraction concentration range. DMSO makes the dominant contribution to the surface potential, and as its bulk concentration increases, the increase in the DMSO contribution approximately balances the reduced water contribution so that the total potential drop remains unchanged.

By starting the simulations from an initial nonequilibrium density profile (zero DMSO surface excess), we are able to study the dynamics of adsorption as a function of bulk concentration. We demonstrate (by comparison with a numerical solution of a diffusion equation) that the time scale (about 1 ns) for the establishment of the equilibrium surface excess is in agreement with diffusion in an external field (the potential of mean force). However, the approach to the equilibrium orientation is much faster.

The model of water/DMSO mixtures presented here is quite simple, and yet it provides a reasonable picture of the surface of these systems. Nevertheless, the importance of the water/DMSO system for many areas of research makes a case for the need to further improve the model potentials. This can be accomplished by including many-body electronic polarizability on both the water and DMSO molecules and by optimizing the water-DMSO interactions beyond the simple mixtures rules. For this purpose, it would be useful to have additional structural and thermodynamics data over a wider concentration range of the mixtures.

ACKNOWLEDGMENT

This work has been supported by a grant from the National Science Foundation (CHE-9628072).

[1] W. J. DeBruyn, J. A. Shorter, P. Davidovits, D. R. Worsnop, M. S. Zahniser, and C. E. Kolb, J. Geophys. Res. **99**, 16927 (1994).
[2] B. B. Damaskin, V. Y. Tyurin, and S. L. Dyatkina, Elektrokhim. **27**, 1358 (1991).
[3] G. Jarzabek and Z. Borkowska, J. Electroanal. Chem. **248**, 399 (1988).
[4] *Dimethyl Sulfoxide*, edited by S. W. Jacobs, E. E. Rosenbaum, and D. C. Woods (Marcel Dekker, New York, 1971).
[5] I. I. Vaisman and M. L. Berkowitz, J. Am. Chem. Soc. **114**, 7889 (1992).
[6] A. Luzar and D. Chandler, J. Chem. Phys. **98**, 8160 (1993).
[7] A. K. Soper and A. Luzar, J. Phys. Chem. **100**, 1357 (1996).
[8] J. Dabkowski, I. Zagórska, M. Dabkowska, Z. Koczorowski, and S. Trasatti, J. Chem. Soc., Faraday Trans. **92**, 3873 (1996).
[9] S. G. Grubb, M. W. Kim, T. Raising, and Y. R. Shen, Langmuir **4**, 452 (1988).
[10] K. B. Eisenthal, Chem. Rev. **96**, 1343 (1996).
[11] D. Zhang, J. H. Gutow, K. B. Eisenthal, and T. F. Heinz, J. Chem. Phys. **98**, 5099 (1993).
[12] Q. Du, E. Freysz, and Y. R. Shen, Science **264**, 826 (1994).
[13] D. S. Karpovich and D. Ray, J. Phys. Chem. B **102**, 649 (1998).
[14] H. C. Allen, D. E. Gragson, and G. L. Richmond, J. Phys. Chem. B **103**, 660 (1999).
[15] K. Wolfrum, H. Graener, and A. Laubereau, Chem. Phys. Lett. **213**, 41 (1993).
[16] A. Luzar, J. Chem. Phys. **91**, 3603 (1989).
[17] M. Matsumoto, Y. Takaoka, and Y. Kataoka, J. Chem. Phys. **98**, 1464 (1993).
[18] M. Tarek, D. J. Tobias, and M. L. Klein, J. Chem. Soc., Faraday Trans. **92**, 559 (1996).
[19] A. Pohorille and M. A. Wilson, J. Phys. Chem. B **101**, 3130 (1997).
[20] K. Kuchitsu and Y. Morino, Bull. Chem. Soc. Jpn. **38**, 814 (1965).
[21] I. Benjamin, in *Modern Methods for Multidimensional Dynamics Compu-*

tations in Chemistry, edited by D. L. Thompson (World Scientific, Singapore, 1998), p. 101.
[22] D. Chandler, *Introduction to Modern Statistical Mechanics* (Oxford University Press, Oxford, 1987).
[23] I. A. Borin and M. S. Skaf, Chem. Phys. Lett. **296**, 125 (1998).
[24] J. D. Jackson, *Classical Electrodynamics* (Wiley, New York, 1963).
[25] I. Benjamin, Chem. Rev. **96**, 1449 (1996).
[26] J. S. Rowlinson and B. Widom, *Molecular Theory of Capillarity* (Clarendon, Oxford, 1982).
[27] I. Benjamin, J. Chem. Phys. **96**, 577 (1992).